Environ. Eng. Res. 2024; 29(2): 230137
https://doi.org/10.4491/eer.2023.137

pISSN 1226-1025
eISSN 2005-968X

Research

Evaluation of atrazine degradation by iron persulfate activation process in aqueous phase using Taguchi approach

Xuyen Thi Hong Luong, Chenju Liang†

Department of Environmental Engineering, National Chung Hsing University, 145 Xingda Road, Taichung 402, Taiwan

Received March 12, 2023 **Revised** May 16, 2023 **Accepted** June 4, 2023

ABSTRACT

Atrazine (ATZ) is one of the most widely used herbicides for the control of annual broadleaf and grassy weeds in the world. Its residual in the environment is of great concern. This research work primarily focused on examining ATZ degradation by the ferrous ion activated persulfate (PS) oxidation process (Fe^{2+}-AP process) and the influence of oxidative parameters on the degradation of ATZ in aqueous phase. The Taguchi Design of Experiment methodology was used to explore the effects of various operational parameters, including ATZ concentration, dosage of Fe^{2+}, dosage of PS, and pH condition (Taguchi L9 orthogonal array). The optimal operational conditions were then determined based on the results of ANOVA statistical analysis. Operational conditions included ATZ at an initial concentration of 5 mg/L, with initial concentrations of 1 mM Fe^{2+}, 10 mM PS, and pH = 3, at 20°C, for a reaction time period of 3 h. The sensitivity of factors for the ATZ degradation followed the decreasing order: PS concentration, pH, ATZ concentration and Fe^{2+} dosage. The results of this study provide useful operational conditions for the Fe^{2+}-AP process, for application to field remediation of ATZ contamination.

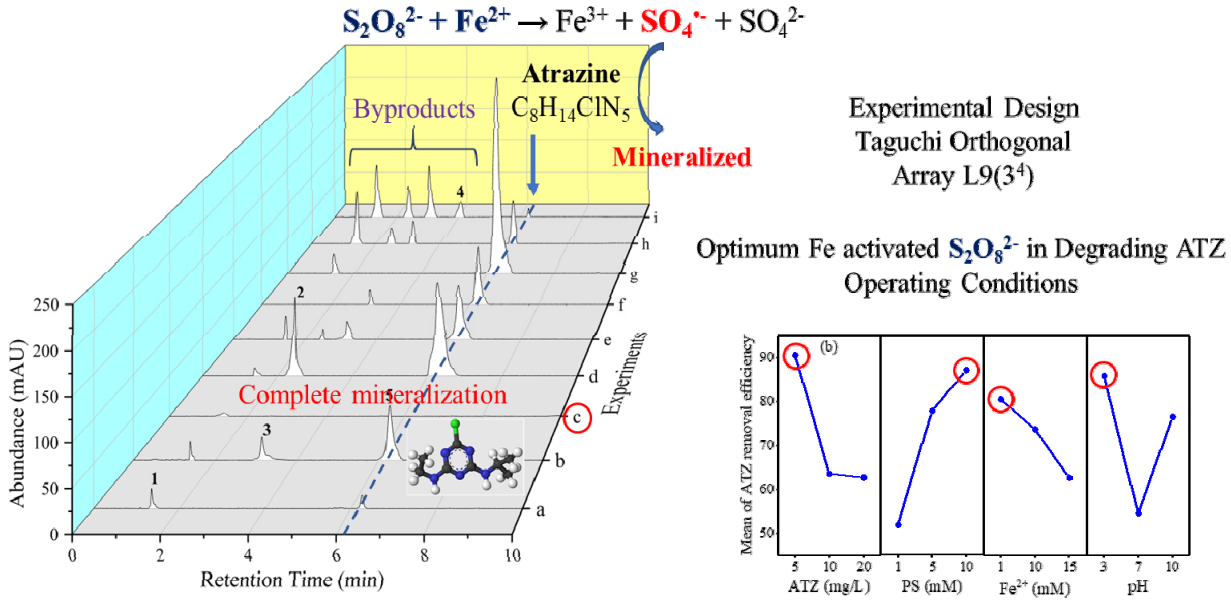
Keywords: Advanced oxidation processes (AOP), Atrazine (ATZ), Ferrous ion activated persulfate (Fe^{2+}-AP), Sulfate radical, Taguchi methodology

This is an Open Access article distributed under the terms of the Creative Commons Attribution Non-Commercial License (http://creativecommons.org/licenses/by-nc/3.0/) which permits unrestricted non-commercial use, distribution, and reproduction in any medium, provided the original work is properly cited.

Copyright © 2024 Korean Society of Environmental Engineers

† Corresponding author
E-mail: cliang@nchu.edu.tw
Tel: +886-4-22856610 Fax:
ORCID: 0000-0002-5028-4668

Graphical Abstract



1. Introduction

Agricultural production is one of the important economic activities in the world, especially in low and middle-income countries, where agriculture contributes significantly to gross domestic product growth. However, an environmental issue associated with agricultural production, that has been of public concern in recent years, is the use of herbicides. The long-term use of large amounts of herbicides has caused contamination of lakes, streams, oceans, groundwater, and surface water, etc. [1]. Atrazine (2-chloro-4-ethylamino-6-amino-s-triazine, ATZ) is one of the most commonly used herbicides for pre and post-emergence control of broadleaf and grassy weeds [2-4]. ATZ was patented in Basel, Switzerland in 1952 [5] and was registered for commercial use in the United States in 1959; afterwards, it was used worldwide [6]. This chemical is, or was, used in agriculture, industries, and households in over 80 countries [7].

The use of ATZ was banned in the European Union in 2004 [8], Germany and Italy in 1991 [9], and the United Kingdom in 1993 [10], but it is still used on a large scale in the United States [11, 12] and in some Asia countries such as Vietnam [13]. ATZ was found to be present in the groundwater [14, 15], surface water [16, 17], and soil [18, 19]. ATZ has been frequently detected in groundwater at a concentration higher than the Maximum Contaminant Level (MCL) of 3 μg/L for drinking water set by the United States Environmental Protection Agency (USEPA) [20]. It has also been reported that ATZ in groundwater wells and rivers were 88 μg/L and 100 μg/L, respectively, in the United States [21, 22] and ATZ in waters directly exposed to agricultural land was as high as approximately 1 mg/L [23]. ATZ can act as an endocrine disruptor in organisms, and its accumulation through the food chain can pose a potential risk to human health and other creatures [8, 24]. Therefore, the investigation of efficient ATZ remediation methods may provide significant environmental benefits.

Various processes are commonly used to treat ATZ, including activated carbon (AC) and biochar adsorption, phytoremediation, and microbial remediation. In a study by Zheng et al., the adsorption capacity of biochar for ATZ and simazine was investigated, revealing that the adsorption rate depends on the particle size of biochar, and the solution's pH. Smaller particle sizes exhibited faster pesticide adsorption compared to larger particles. Additionally, at pH levels below 7, the adsorption affinity for both ATZ and simazine decreased with increasing pH. However, at pH levels above 7, the adsorption affinity for these two pesticides remained stable. The study suggested that biochar has the potential to mitigate pesticide residue in aquatic environments [25]. Shao et al. examined a membrane filtration system with an added thin layer of adsorbent materials, such as anion exchange resin (AER), powdered activated carbon (PAC), or SiO_2, for filtering ATZ from a solution. A control group using an unmodified gravity-driven membrane (GDM) system was also conducted. After four days of operation, the unmodified GDM system showed the lowest ATZ removal efficiency (3.7%), while the PAC adsorbent GDM system achieved the highest ATZ removal efficiency (28.5%). Furthermore, the ATZ removal efficiencies of the SiO_2 filtration GDM system and AER treatment GDM system were 5.9% and 11.6%, respectively. The study concluded that incorporating a pre-treatment adsorbent layer onto the GDM system could enhance water treatment quality by removing micropollutants like ATZ [26].

Sánchez et al. conducted a study to assess the uptake capacities of four plant species, namely tall fescue (*Festuca arundinacea*), ryegrass (*Lolium perenne*), barley (*Hordeum vulgare*), and maize (*Zea mays*), in removing ATZ from contaminated soil. The initial concentrations of ATZ in the soil were 2, 5, and 10 mg/kg. After 16 days, approximately 63.1-78.2% of ATZ in unplanted pots had

degraded, while planted pots exhibited removals of approximately 88% of ATZ from the soil. The findings demonstrated that phytoremediation with these plants led to the accumulation of ATZ in plant tissues, such as shoots and roots, as well as the generation of metabolites like deisopropylatrazine and deethylatrazine [27]. Phytoremediation technology offers several advantages, including cost-effectiveness, ease of operation, and environmentally friendly nature. However, the accumulation of parent compounds and metabolites in plants is a contaminant transfer mechanism, not a contaminant destruction mechanism. Therefore, the search for suitable plant species that can facilitate degradation and transform pollutants into environmentally benign forms remains a challenge. Numerous researchers have achieved success by employing isolated microbial strains that utilize ATZ as a nitrogen source and produce carbon dioxide through microbial bioremediation [28]. Microbial bioremediation shares similar advantages with phytoremediation. However, these bio-processes are highly influenced by environmental variables, such as temperature, pH level, salinity, and nutrient availability. Therefore, there is a need to identify bacterial strains that can withstand harsh environments and explore gene-editing technologies to enhance the assimilation efficiency of bacteria.

Advanced oxidation processes (AOPs) have received considerable attention for the destruction of organic contaminants such as pesticides, herbicides, surfactants, pharmaceuticals, and endocrine-disrupting chemicals, by drinking water treatment systems, and wastewater treatment systems [29-31]. AOPs may include photo peroxidation, chemical, sonochemical and electrochemical processes [32]. These processes are based on the generation of powerful reactive species such as hydroxyl radical ($^{\bullet}OH$), sulfate radical ($SO_4^{\bullet-}$), superoxide radical ($O_2^{\bullet-}$), hydroperoxyl radical ($HO_2^{\bullet}$) or singlet oxygen ($^1O_2$), to oxidize a wide range of organic contaminants [2-4]. One of the AOPs, persulfate (PS) ($S_2O_8^{2-}$) activation to generate $SO_4^{\bullet-}$, has been recognized as effective for degrading environmental contaminants [33]. Among common PS activation processes, transition metal activation, e.g., ferrous ion (Fe^{2+}), requires less activation energy (12 kcal/mole) to break down the O-O bond for $SO_4^{\bullet-}$ generation (Eq. (1)) than thermal activation (33.5 kcal/mole) [33-37]. The Fe^{2+} activated PS process (Fe^{2+}-AP) exhibits the potential to remediate ATZ contamination. Therefore, this research focused on studying the performance of $SO_4^{\bullet-}$ in degrading ATZ using the Fe^{2+}-AP process under different experimental conditions in the aqueous phase. The effects of different operating parameters such as the ATZ concentration, dosages of PS, and Fe^{2+}, initial pH, and temperatures on the ATZ degradation performance were studied.

$$S_2O_8^{2-} + Fe^{2+} \rightarrow Fe^{3+} + SO_4^{\bullet-} + SO_4^{2-} \ (k = 2.0 \times 10^1\ M^{-1}s^{-1}) \quad (1)$$

The research group led by Samy et al. conducted a study exploring the use of a combination of photocatalysts and adsorption systems to remove 1,4 dioxane. They employed copper/iron-doped zinc oxide (Cu-Fe-ZnO) in a solar photo-oxidation reactor to generate $^{\bullet}OH$ radicals, which effectively decomposed 1,4 dioxane present in hazardous landfill leachate. The findings indicated that the photocatalytic activity of ZnO was enhanced by the adsorption behavior of pollutant molecules. This efficient removal of 1,4 dioxane using a small amount of catalyst and a short reaction time holds promise for industrial discharge treatment, ultimately reducing treatment costs [38]. In another study by the same research group [39], the degradation of carbofuran, a carbamate pesticide derivative, was evaluated through heterogeneous activation of PS using a novel composite AC derived from the water hyacinth plant, zinc oxide, and nano-magnetite. The study revealed that the degradation mechanism of carbofuran involved the active participation of $SO_4^{\bullet-}$ and $^{\bullet}OH$ radicals through a photo-Fenton-like reaction.

Samy et al. employed toner waste as a precursor to produce an iron oxide-nanographene nanohybrid, which effectively activated PS and facilitated the efficient degradation of pesticides, including diazinon [40]. In a separate study, Mensah et al. assessed the performance of three solid iron wastes derived from different steel industries as activators of PS in degrading dye solutions. Remarkably, the degradation efficiencies of various dye solutions such as Congo red, methyl red, acid blue-25, and methylene blue were nearly complete within a short reaction time of less than one hour [41]. These results collectively demonstrate the potential of transition metal activation as a promising approach to generate oxidant radical species and effectively treat a wide range of organic contaminants using PS.

Obtaining the optimum removal efficiency of groundwater contaminants from soil is a challenging task that requires multiple separate experiments to determine the process parameters. However, the Taguchi orthogonal array design of the experimental technique can greatly assist in analyzing the variables of the pollution treatment process and achieving the best possible design results. This technique is highly effective in evaluating and optimizing processes that encompass multiple input parameters [42]. One of its notable advantages is that it enables process optimization with minimal trials and experiments. The Taguchi technique is a well-established, cost-effective approach for optimizing product quality and reliability, based on the principles of the Taguchi Design of Experiment (DOE) Methodology. Although widely applied in various fields such as infrastructure [43], dental science [44], welding [45], and energy systems [46], its application in the treatment of herbicides in wastewater and groundwater remains relatively unexplored. Furthermore, despite its potential to reduce testing costs and time, only a few studies have utilized this approach in combination with advanced oxidation processes for treating residual herbicides, such as ATZ in groundwater. Therefore, the specific objectives of this research were (1) to investigate the effects of various experimental conditions on ATZ degradation by the Fe^{2+}-AP process in the aqueous phase, using the Taguchi Methodology and (2) to investigate the effects of PS activation temperature on ATZ degradation under optimum experimental conditions.

2. Materials and Methods

2.1. Chemicals and Materials

The chemicals used were purchased from the following sources. ATZ ($C_8H_{14}ClN_5$, min. 97.4%) was purchased from Riedel-dehaën. Sodium persulfate (SPS) ($Na_2S_2O_8$, min. 99%) was purchased from

Merck. Ferrous sulfate ($FeSO_4 \cdot 7H_2O$, min. 99%), sodium bicarbonate ($NaHCO_3$, min. 99.7%), and phosphoric acid (H_3PO_4, min. 86.5%) were purchased from J.T. Baker. Sodium carbonate (Na_2CO_3, min. 99.5%) was purchased from Fluka. Sodium hydroxide (NaOH, min. 99%), sulfuric acid (H_2SO_4, min. 95%), and potassium hydrogen phthalate ($KHC_8H_4O_4$, min. 99.5%) were purchased from Aldrich. Methanol (CH_3OH, min. 99.5%) was purchased from Macron Fine Chemicals. Potassium iodide (KI, min. 99.5%) was purchased from Union Chemical Works. FerroVer Iron Reagent (for total iron analysis) and Ferrous Iron Reagent (for Fe^{2+} analysis) were purchased from Hach Company. Water used was prepared by reverse osmosis (RO) purification system (Model: Sky water XL-300A).

2.2. Taguchi's Orthogonal Experimental Design and Experimental Procedure

2.2.1. Taguchi's orthogonal experimental design

Taguchi methodology is a statistical method for finding the best experimental conditions and best quality performance with fewer experiments. In this study, Taguchi L9 (3^4) orthogonal array was selected to determine the effect of four factors, i.e., concentration of ATZ (mg/L), dosage of ferrous ion (mM), dosage of PS (mM), and initial pH condition. The Taguchi L9 experimental design, with four different factors, and three levels for each factor, are shown in Table 1. The ATZ removal efficiency (%) was calculated under each specified experimental condition.

Taguchi orthogonal Array generates the signal-to-noise (S/N) ratio for measuring effects of the response variables, where the unit of S/N ratio is the decibel (dB). The larger the S/N ratio, the greater the ATZ removal efficiency. The raw data were converted into a corresponding S/N ratio in accordance with Eq. (2). Additionally, the contribution percentage of each individual parameter was computed using Analysis of Variance (ANOVA).

$$\frac{S}{N}(dB) = -10 \log\left(\frac{1}{n}\sum_{i=1}^{n}\frac{1}{y_i^2}\right) \quad (2)$$

where n is the number of experiments, and y_i is the ATZ removal efficiency of each experiment.

2.2.2. Experimental procedure

A 25 mg/L stock-solution of ATZ was prepared by adding ATZ to a 2 L borosilicate glass reservoir, filling with RO water, and stirring at room temperature (25±2°C) until complete dissolution (approximately 24 h) was achieved. This ATZ stock-solution was diluted to obtain aliquots of the required initial concentrations. Stock solutions of ferrous sulfate were prepared separately at different initial concentrations. Upon mixing ATZ and Fe^{2+} stock solutions to achieve the designated concentration levels in a series of 250 mL conical flasks for different experiments, initial pH values were adjusted using 0.1 M H_2SO_4 or 0.1 M NaOH solutions. The pre-weighted SPS powders were then added into each flask. Thereafter, each resulting flask solution was distributed into four different 60 mL amber glass bottles and zero head space was maintained in reaction bottles. All reaction bottles were placed in a temperature-controlled chamber at 20°C.

During the study, samples were taken at specific time intervals (2 mins, 0.5, 1, 2, and 3 h) from two reaction bottles. From each reaction bottle, sample solutions were withdrawn to analyze the concentrations of ATZ, PS, Fe^{2+}, total dissolved iron (T-Fe), total organic carbon (TOC), oxidation-reduction potential (ORP), and pH. To prepare the samples for analysis, the withdrawn solution was filtered using a gas-tight syringe equipped with a stainless syringe holder and a 0.2 μm PTFE membrane filter. This filtration step was performed to ensure the removal of any particulate matter or impurities before conducting the analysis for ATZ, TOC, PS, and Fe. Control experiments with only ATZ, only PS, and only Fe^{2+}, were also conducted in parallel for comparison. When the operational conditions were determined, further experiments were run to determine the effect of reaction temperature (10, 20 and 40°C). All experiments were conducted in duplicate and averaged data with relative error range were presented.

2.3. Analytical Methods

The concentration of ATZ was determined using a high-performance liquid chromatography system (HPLC, PerkinElmer Fexar LC) equipped with a photodiode array detector (PDA). A Brownlee SPP C18 column (4.6 × 150 mm, particle size 2.7 μm) was used for analyte separation. Methanol and RO water, mixed at a ratio

Table 1. Experimental Design of L9 Orthogonal Array

Levels		Factors			
		ATZ (mg/L)	PS (mM)	Fe^{2+} (mM)	pH
Level 1		5	1	1	3
Level 2		10	5	10	7
Level 3		20	10	15	10
Experiments	a	5	1	1	3
	b	5	5	10	7
	c	5	10	15	10
	d	10	1	10	10
	e	10	5	15	3
	f	10	10	1	7
	g	20	1	15	7
	h	20	5	1	10
	i	20	10	10	3

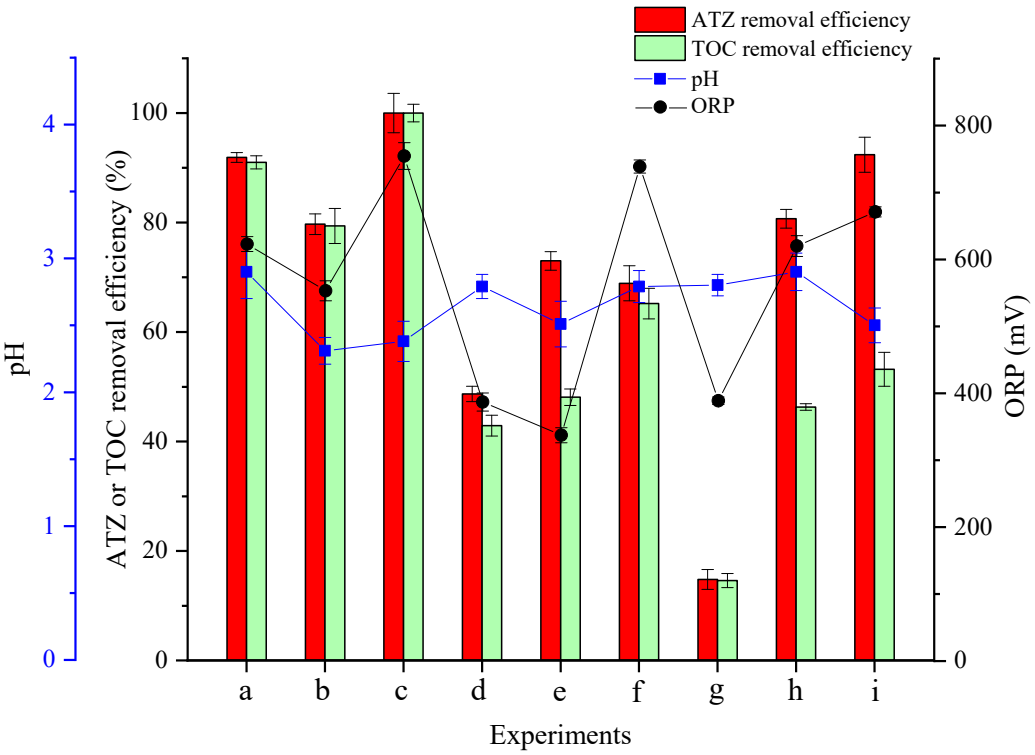


Fig. 1. The ATZ and TOC removal efficiency, pH, and ORP under different experimental conditions. (a) to (i) based on the experimental design of L9 orthogonal array.

of 60/40 (v/v), was used as the HPLC mobile phase with a flow rate of 0.8 mL min^{-1}. The HPLC detector was set to detect ATZ at a wavelength of 224 nm. PS anion was determined using a spectrophotometric method (Liang et al.) and measured with a UV-vis spectrophotometer (HACH DR/2400) at 400 nm. The total dissolved iron and ferrous ion concentrations were colorimetrically measured using a HACH DR/2400 spectrophotometer at 510 nm in accordance with the HACH methods 8146 and 8008, respectively. The pH was measured using a pH/ISE meter (Hanna Instruments HI 5222) equipped with a pH combination electrode LE 407. The ORP of solutions were measured by a pH/ISE meter (Hanna Instruments HI 5222) equipped with a redox combination electrode (Mettler Toledo Inlab 507 Redox). The concentration of TOC was measured using a TOC analyzer (Aurora 1030 W, O.I. Analytical) by a wet oxidation technique.

3. Results and Discussion

3.1. Fe^{2+}-AP Process on ATZ Degradation in Aqueous Phase

Degradations of ATZ by Fe^{2+}-AP process were evaluated using a Taguchi L9 (3^4) orthogonal array with different experimental conditions, and the results are shown in Fig. S1, Supplementary materials (SM). As expected, the Fe^{2+}-AP process generates $SO_4^{\bullet-}$, resulting in rapid degradation of ATZ at an early stage (2 min). Thereafter, the degradation reaction rate decreased. The degradation efficiency of ATZ (C/C_0) reached 50-70% in experiments b, e, f, and h during the course of a 3-h reaction, while the elevated efficiency of 85-100% was observed in experiments a, c, and i (as shown in Fig. 1). These results demonstrated that ATZ can be effectively degraded by the Fe^{2+}-AP process with the assistance of active $SO_4^{\bullet-}$ formed. The ATZ degradation is comprised of several steps. The PS decomposition occurred (Eq. (1)) during the first 2 min of the oxidation process, and thereafter the degradation of ATZ seemed to halt, as shown in Fig. S2 (SM). Fe^{2+} can rapidly be transformed to Fe^{3+}, which may produce ferric hydroxide ($Fe(OH)_3$) (Eq. (3)). However, as seen in Fig. S2 (SM), the concentration of T-Fe was comparable to the initial Fe^{2+} concentration, indicating $Fe(OH)_3$ dissolved as Fe^{3+} at acidic pH ~ 3 (Eq. (4)) (see Fig. S3) in the Fe^{2+}-AP process [47]. It should be noted that the activation of PS by $Fe(OH)_3$ or Fe^{3+} might be negligible [48]. Moreover, to some extent, the oxidation reaction toward ATZ may be inhibited by excess PS and $SO_4^{\bullet-}$ generated, due to competitive reactions as shown in Eqs. (5) and (6) [49]. Although ATZ can be degraded by the Fe^{2+}-AP process, the degradation efficiency of ATZ in experiments d and g only reached 48.7 % and 14.8 %, respectively, within 3 h, where the PS dosage of 1 mM was limiting and depleted in the presence of excess of Fe^{2+} (i.e., 10 and 15 mM). Samy et al. conducted a study on the utilization of a synthesized iron oxide-nanographene nanohybrid for activating persulfate in the degradation of methylene blue dye [40]. They emphasized the importance of optimizing the operating parameters for the sulfate radical-based oxidation process in practical applications. The researchers also highlighted that the reduction of ferrous ion could potentially serve as a limiting factor in the

activation of persulfate. In another investigation by Samy et al., zinc oxide/water hyacinth-based activated carbon and nano-magnetite nanohybrid were employed as activators [39]. The study revealed that increasing the concentration of persulfate generally led to enhanced degradation efficiency of the carbofuran contaminant. This improvement was attributed to the increased production of sulfate and hydroxyl radicals. It should be noted that a theoretical Fe^{2+}/PS molar ratio of 2 is required in accordance with Eq. (7).

$$Fe^{2+} + S_2O_8^{2-} + 3H_2O \rightarrow Fe(OH)_3 + SO_4^{\bullet-} + SO_4^{2-} + 3H^+ \quad (3)$$

$$Fe(OH)_3 + 3H^+ \rightarrow Fe^{3+} + 3H_2O \quad (4)$$

$$SO_4^{\bullet-} + S_2O_8^{2-} \rightarrow S_2O_8^{\bullet-} + SO_4^{2-} \ (k = 1.5\times10^3 - 1.2\times10^6\ M^{-1}s^{-1}) \quad (5)$$

$$SO_4^{\bullet-} + SO_4^{\bullet-} \rightarrow S_2O_8^{2-} \ (k = (1.6\text{-}8.1)\times10^8\ M^{-1}s^{-1}) \quad (6)$$

$$S_2O_8^{2-} + 2Fe^{2+} \rightarrow 2Fe^{3+} + 2SO_4^{2-} \ (k = 3.1\times10^4\ M^{-1}s^{-1}) \quad (7)$$

Fig. S2 (SM) presents the concentration variation of PS, Fe^{2+}, and T-Fe during the course of the Fe^{2+}-AP process under different experimental conditions. The dosages of two factors, PS and Fe^{2+}, were the governing reagents in the Fe^{2+}-AP process. PS was quickly decomposed in the Fe^{2+}-AP system for all experiments, and then the degradation rate slowed or nearly halted. In experiments d and g, the initial dosages of PS were 1 mM and Fe^{2+} were 10 and 15 mM, respectively (as shown in Figs. S2(d) and (g) (SM)). It can be seen that complete PS decompositions were attained, indicating that the applied Fe^{2+}/PS molar ratio is much greater than the theoretical ratio of 2 (e.g., 10 and 15 in experiments d and g, respectively). When increasing the dosages of PS in this system, ATZ removal efficiency was not accordingly increased. For example, as seen in experiments a and b, when increasing the PS concentration from 1 mM (experiment a) to 5 mM (experiment b), the removal efficiency of ATZ was reduced from 87.4 % to 55.2 %, respectively, with the same initial ATZ concentration (5 mg/L). The ATZ degradation was not only affected by the dosage of PS but also by other factors such as the dosage of Fe^{2+} and pH condition. It was found from Fig. S2 (SM) that the Fe^{2+} concentrations were significantly decreased by about 71%-100% as soon as the reaction started, but the T-Fe in the system had minor changes and remained at the initial concentration levels. These results demonstrated that Fe^{2+} ions were rapidly and mostly converted to Fe^{3+} and limited Fe^{2+} were available for further activation. Hence, oxidative degradations of ATZ and PS decomposition happened and then halted as soon as the reaction started. However, the T-Fe appeared only slightly decreased from the Fe^{2+} concentration level initially added. Meanwhile, the T-Fe was mainly present in the form of Fe^{3+}, which remained in dissolved

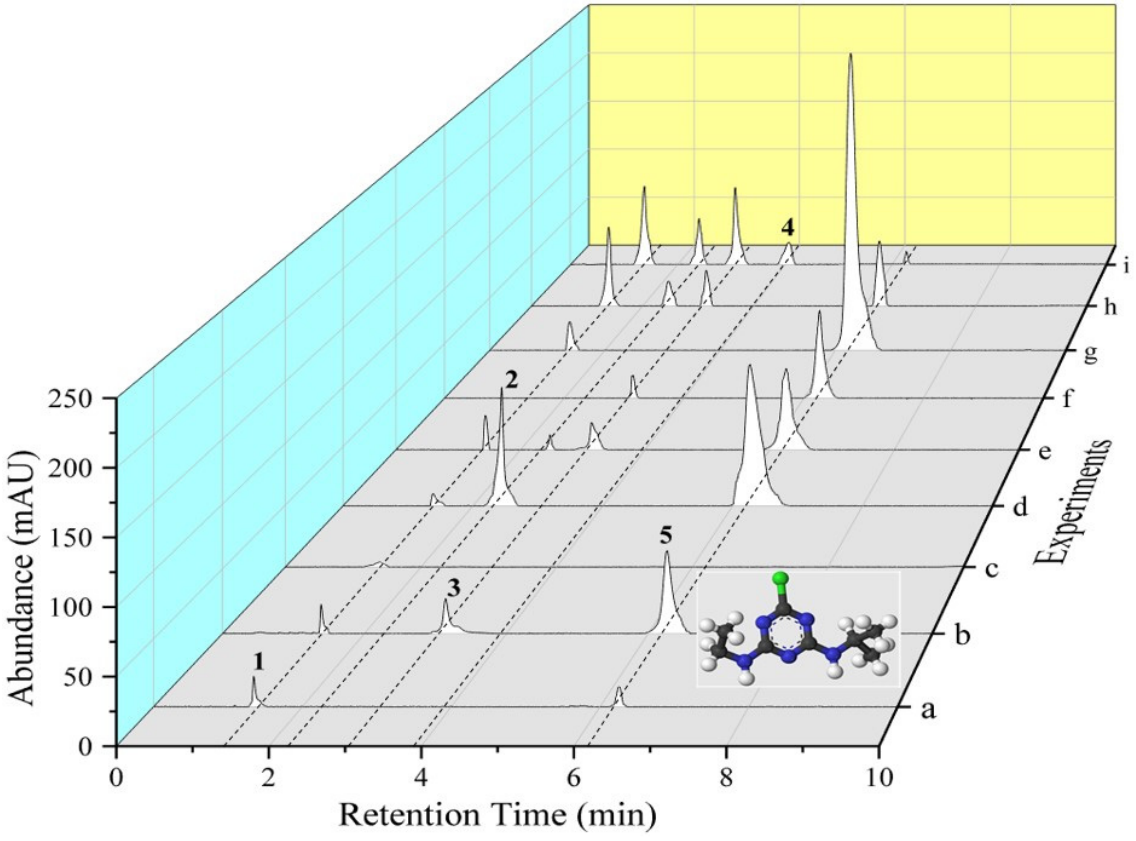


Fig. 2. HPLC-PDA Chromatography spectrum of ATZ and four degradation intermediates after 3 h of reaction time under different experimental conditions. (a) to (i) based on the experimental design of L9 orthogonal array.

form, instead of iron oxide precipitates, and this could be due to the acidic pH condition (e.g., < pH 3). The variations of pH during reactions are presented in Fig. S3 (SM). It can be seen that regardless of the initial pH, pH decreased once the reaction started.

The investigation of effects of varying pH conditions on the degradation of ATZ by the Fe^{2+}-AP process was carried out at pH 3, 7, and 10. The pH levels changed mainly at the beginning of the reaction (2 min), and afterwards the pH did not change (see Fig. S3 (SM)). The solution with an initial pH value of 3.0 was slightly changed to 2.5 to 2.9 after 3 h, while the initial solution pH of 7 and 10 significantly decreased to 2.3 - 2.9 and 2.4 - 2.8, respectively, after 3 h. The decrease in pH value is a natural behavior of PS, which could react with water to produce hydrogen sulfate (HSO_4^-) and further release H^+ in accordance with Eqs. (8) and (9), respectively, [50] resulting in a more acidic pH. Additionally, upon PS activation, $SO_4^{\bullet-}$ generated could react with OH^- or H_2O to form $^{\bullet}OH$ by consuming OH^- and generating H^+ as shown in Eqs. (10) and (11), respectively [50, 51]. Both $SO_4^{\bullet-}$ and $^{\bullet}OH$ may coexist in the system and transfer electrons from ATZ to form ATZ intermediate organic radical ($ATZ^{\bullet}$), postulated as shown in Eq. (12). Moreover, all oxidizing species ($S_2O_8^{2-}$, $SO_4^{\bullet-}$ and $^{\bullet}OH$) could initiate a series of chain reactions with $ATZ^{\bullet}$ and then be further degraded, as shown in Eq. (13).

$$S_2O_8^{2-} + H_2O \rightarrow 2HSO_4^- + 0.5O_2 \quad (8)$$

$$HSO_4^- \rightarrow SO_4^{2-} + H^+ \ (pK_a = 1.99) \quad (9)$$

$$SO_4^{\bullet-} + OH^- \rightarrow SO_4^{2-} + {}^{\bullet}OH \ (k = 6.5 \times 10^7\ M^{-1}\ s^{-1}) \quad (10)$$

$$SO_4^{\bullet-} + H_2O \rightarrow SO_4^{2-} + H^+ + {}^{\bullet}OH \ (k\ [H_2O] < 2 \times 10^{-3}\ s^{-1}) \quad (11)$$

$$SO_4^{\bullet-} \text{ or } {}^{\bullet}OH + ATZ \rightarrow ATZ^{\bullet} + \text{byproducts} \quad (12)$$

$$S_2O_8^{2-} \text{ or } SO_4^{\bullet-} \text{ or } {}^{\bullet}OH + ATZ^{\bullet} \rightarrow \text{byproducts} \quad (13)$$

After mixing Fe^{2+} and PS, ORP values increased immediately (Fig. S3 (SM)), for example, the ORP remained around 400 mV in experiments d, e, and g, and 600 mV in experiments a, b, h, and i. The ORP value in experiments c and f increased most significantly to over 700 mV after 2 min. The observed ORP variation may not be indicative of true redox capacity because absolute ORP must account for hydrogen ion activity [52]. Nonetheless, the observed increased ORP could still indicate that the Fe^{2+}-AP system created a strong oxidizing condition.

TOC removal reflects the extent of mineralization of organic compounds. The concentration of TOC in the Fe^{2+}-AP system under different experimental conditions was shown in Fig. S4 (SM). It was observed that TOC concentration variations during the course of reaction were comparable to those of ATZ degradation. The removal efficiencies of ATZ and TOC, and the ratio between TOC and ATZ removal efficiency (ΔTOC/ΔATZ) are summarized in Table 2. In experiment c, the maximum ΔTOC/ΔATZ achieved is equal to 1.00, which could be related to the complete removal of ATZ at the end of the treatment. However, the ΔTOC/ΔATZ is less than 1.00 in other experiments. Especially, the minimum ΔTOC/ΔATZ is 0.57 after 3 h while ATZ removal efficiency is 80.7% in experiment h. These results indicate that ATZ could be transformed into intermediate products. On the basis of five compounds detected by HPLC/PDA, chromatograms as illustrated in Fig. 2, peak#1 to #4 appeared to be ATZ (peak#5) degradation byproducts. These unidentified byproduct peaks remained in the reaction solution would contribute to the TOC content. Samy et al. incorporated TOC as a parameter to assess the effectiveness of treating 1,4-dioxane in hazardous landfill leachate [38]. The utilization of TOC measurements allowed them to determine the degree of mineralization or breakdown of organic compounds. Evaluating TOC removal efficiency enabled them to distinguish between physical adsorption, where the contaminants are merely trapped or absorbed, and chemical degradation, where the contaminants are chemically transformed and broken down during the persulfate activation process. TOC serves as a valuable tool in gauging the extent of organic compound degradation and provides insights into the overall removal of organic pollutants from the leachate. By monitoring the changes in TOC concentration throughout the treatment process, they were able to ascertain the effectiveness of persulfate activation in mineralizing the organics present in the hazardous landfill leachate. Identification of these intermediate products requires further evaluation to ensure no harmful products generated during the course of reaction. It can be seen in Fig. 2 that ATZ (peak #5) was completely degraded in experiment c and no byproducts were formed, corresponding to complete removal of TOC, as shown in Fig. 1.

3.2. Analysis of ATZ Removal Performance

In this study, the ATZ removal efficiency by the Fe^{2+}-AP process and associated influences of experimental parameters were evaluated via ANOVA methods. The aim of this study was to achieve the highest ATZ removal efficiency as possible. Therefore, the characteristic of Signal to Noise ratio (S/N) used in this research was set as The-Larger-The-Better. S/N ratio analysis was conducted in order to differentiate the effect of factors including, concentration of ATZ, PS and Fe^{2+} dosages, and pH values. All four control factors with different levels of values under 9 experimental conditions and their corresponding S/N ratio values are tabulated in Table 2. It can be seen from Table 2 that, as the ATZ removal efficiency increases, the S/N ratio increases among these 9 experiments. The highest ATZ removal efficiency (100.0 %), with the highest S/N ratio (40.00 dB) was obtained in experiment c. Similarly, the lowest ATZ removal efficiency (14.8 %) corresponded to the lowest S/N ratio (23.43 dB) in experiment g.

Tables S1 and S2 (SM) present averaged responses of S/N ratio and ATZ removal efficiency for each level, respectively. The S/N ratio of the ATZ concentration factor was highest at level 1 (5 mg/L) (39.10 dB) and the higher the ATZ concentration (level 3: 20 mg/L) the lower the S/N ratio. In addition, the averaged ATZ removal efficiency at ATZ concentration levels 1 to level 3 decreased from 90.5% to 62.7%, respectively. These results showed that changing the concentration of ATZ would affect the removal efficiency. Moreover, both the S/N ratio and averaged ATZ removal efficiency increased with the increase of PS concentration.

Table 2. ATZ and TOC Removal Efficiencies, and ΔTOC/ΔATZ under Different Experimental Conditions and Corresponding S/N Ratio Values.

Experiments	ATZ removal efficiency (%)	TOC removal efficiency (%)	ΔTOC/ΔATZ	S/N Ratio
a	91.9	91.0	0.99	39.27
b	79.7	79.4	0.99	38.03
c	100.0	100.0	1.00	40.00
d	48.7	42.9	0.88	33.75
e	73.0	48.1	0.66	37.27
f	68.9	65.2	0.95	36.77
g	14.8	14.6	0.99	23.43
h	80.7	46.3	0.57	38.14
i	92.4	53.2	0.58	39.32

To study the effect of Fe^{2+} dosages, it was seen that at the lowest concentration of Fe^{2+} (1 mM), the S/N ratio is highest with 38.06 dB, while, at the highest concentration of Fe^{2+} (15 mM), the S/N ratio is lowest with 33.57 dB (Table S2 (SM)). The ATZ removal efficiency was reduced with increasing iron concentration (from 80.5% (level 1) to 62.6% (level 3) in the Fe^{2+}-AP process, likely due to excess Fe^{2+} scavenging $SO_4^{\bullet-}$ and $^{\bullet}OH$ [52, 53].

A decrease in the S/N ratio of ATZ removal was found when initial pH increased from 3 to 10 (e.g., 38.62 dB and 37.30 dB at pH 3 and 10, respectively). $SO_4^{\bullet-}$ can be converted to $^{\bullet}OH$ at higher pH as shown in Eq. (10). Mechanisms of $SO_4^{\bullet-}$ and $^{\bullet}OH$ reaction mechanisms with organics are likely different. For example, $SO_4^{\bullet-}$ attacks organic compounds primarily through the processes of electron transfer and hydrogen atom abstraction, while $^{\bullet}OH$ mostly abstracts H from C-H, N-H, or O-H bonds, and adds onto C=C double bonds, or aromatic rings [54]. However, when initial pH is greater than 4.0, Fe^{2+} would form less reactive $FeOH^+$ and $Fe(OH)_2$ species in solution (as shown in Eqs. (12) and (13))

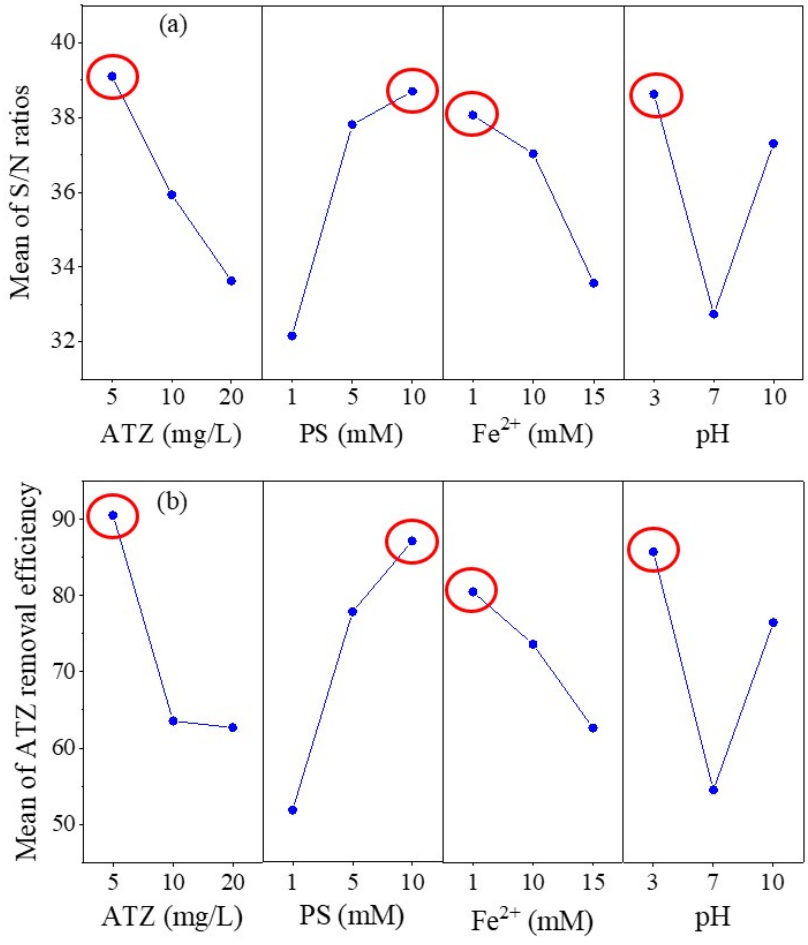


Fig. 3. Main effect plots for means of (a) S/N ratio and (b) ATZ removal efficiency corresponding to each specific factor level.

[55]. Even though elevated pH condition (e.g., > 7) may induce more $^{\bullet}OH$ formation, basic pH may limit effective Fe^{2+} for PS activation due to formation of $FeOH^{+}$ and $Fe(OH)_2$ species. Therefore, in general, acidic pH is the preferable condition for the Fe^{2+}-AP process for destroying ATZ in solution. According to the findings of Mensah et al., an acidic condition was found to promote iron dissolution, resulting in increased availability of Fe^{2+} ions [41]. This increased availability of Fe^{2+} ions is crucial for the activation of persulfate, which in turn leads to the generation of radicals necessary for the degradation of organic compounds.

$$Fe^{2+} + H_2O \rightarrow FeOH^{+} + H^{+} \quad (14)$$

$$FeOH^{+} + OH^{-} \rightarrow Fe(OH)_2 \quad (15)$$

For this study, The-Larger-The-Best was used to evaluate efficiency of ATZ removal in the Fe^{2+}-AP process. Hence, as the delta value of the S/N ratio increases, the ATZ removal efficiency is also expected to increase. In this approach, optimal variables were obtained by sorting delta values in order to discover the significance of factors. A higher delta value indicates a significant influence of the variable on the whole experimental study. The plots of S/N ratio and averaged ATZ removal efficiency versus the factor levels ATZ concentration, dosage of PS, dosage of Fe^{2+}, and pH were shown in Figs. 3(a) and (b), respectively. It was suggested that ATZ concentration, dosage of Fe^{2+}, and pH have the highest values of S/N ratio and ATZ removal efficiency at level 1, whereas dosage of PS has a highest value at level 3. Thus, it can be concluded that the optimal operational conditions are initial concentrations of ATZ = 5 mg/L (level 1), Fe^{2+} = 1 mM (level 1), PS = 10 mM (level 3), and pH = 3 (level 1). After comparing the treatment efficiency of ATZ in this study with other studied processes that have reported treatment efficiencies, such as 3.7-28.5% through AC adsorption [26], 78.2-88.6% through phytoremediation [27], and 31.2-46.0% through microbial remediation [56], it becomes evident that the Fe^{2+}-AP process has the potential to be more effective in treating ATZ contamination.

3.2.1. Analysis of variance (ANOVA)

ANOVA was performed to determine the contribution of each factor in the Fe^{2+}-AP process and the results are given in Table 3. Contributions were calculated in accordance with the following Eq.:

$$\text{Contribution (\%)} = \frac{SS_A}{SS_T} \times 100\% \quad (16)$$

where SS_A is the sum of square of a variable (e.g., factor A) and SS_T is the total sum of squares

In Table 3, the percentage contribution of each factor for degradation of ATZ followed the order: dosage of PS, pH, ATZ concentration, and dosage of Fe^{2+} by 35.8 %, 27.0 %, 21.4 %, and 15.7 % respectively. Therefore, it can be suggested that the dosage of PS is the most important factor, and dosage of Fe^{2+} is the least important factor for ATZ degradation by the Fe^{2+}-AP process.

3.2.2. Confirmation experiment

A confirmation experiment was conducted to validate the results and levels of significant input factors for the optimal operational conditions. Based on the prediction of optimum operational conditions, the ATZ concentration at level 1 (5 mg/L), dosage of PS at level 3 (10 mM), dosage of Fe^{2+} at level 1 (1 mM), and pH at level 1 (pH 3) were evaluated. The treatment efficiency predicted by Taguchi methodology was 100% (see Table S3 (SM) for tabulated experimental conditions and associated calculation) and the efficiency obtained experimentally showed complete ATZ degradation and 91.0% TOC removal under optimized conditions. The results of the confirmation experiment imply that the determined Fe^{2+}-AP process operational design can be suitably applied for ATZ removal.

Table 3. ANOVA Results for Degradation of ATZ by the Fe^{2+}-AP Process.

Factors	DOF[(1)]	SS	Contribution (%)
ATZ	2	45.26	21.4
PS	2	75.71	35.8
Fe^{2+}	2	33.26	15.7
pH	2	57.02	27.0
Total	8	211.25	100.0

[(1)]DOF: degree of freedom

3.2.3. Effects of temperatures on ATZ degradation in the Fe^{2+}-AP process

Temperature was further considered as another factor that would affect the PS activation (Eq. (15)). Therefore, degradations of ATZ under previously determined optimal experimental conditions at various system temperatures of 10, 20, and 40°C were evaluated. When the temperature increased from 10°C to 20°C, the ATZ degradation was increased from 73 % to 88 % at 2 min, and reached 100 % after 30 min at 20°C (see Fig. S5 (SM)). When the temperature increased to 40°C, ATZ was completely removed in the initial stage (2 min). It appeared that the Fe^{2+}-AP process with thermal energy input resulted in aggressive ATZ degradation.

$$S_2O_8^{2-} + \text{heat} \rightarrow 2SO_4^{\bullet-} \text{ (Thermal activation)} \quad (17)$$

(k = 1.0 × 10^{-7} s^{-1} (25°C) or 5.7 × 10^{-5} s^{-1} (70°C)) [57]

4. Conclusions

In this study, Taguchi DOE was employed to investigate the effect of four experimental factors, i.e., ATZ concentration, pH, dosages of PS and Fe^{2+}, with 3 levels for each factor, on ATZ degradation by the Fe^{2+}-AP process in the aqueous phase. This study demonstrated that ATZ can be effectively degraded by the Fe^{2+}-AP process and the optimal conditions were ATZ concentration = 5 mg/L, Fe^{2+} = 1 mM, PS = 10 mM, and pH = 3. Degradation was achieved within a 3 h reaction. Based on the ANOVA analytical results, the dosage of PS exhibited the greatest contribution of 36%. Moreover, the results from the S/N values, and mean of ATZ removal efficiency for different factors, showed that the contribution of each experimental factor was in the order of dosage of PS > pH > ATZ concentration > dosage of Fe^{2+}. Temperature is also a factor that affects the Fe^{2+}-AP process and can significantly accelerate ATZ degradation. It is important to note that the parameters evaluated in this study did not include all environmental variables,

such as the effects of anions (e.g., chloride, (bi)carbonates), natural organic matter, soils, sediments, and other relevant factors. Therefore, while the study provides optimal operational conditions for the Fe^{2+}-AP process, it is crucial to conduct further evaluations considering these environmental conditions before implementing the process for field-scale remediation. It is also worth noting that a model analysis can be conducted to explore the treatment of different concentrations of ATZ in practical applications. Such an analysis would help determine the optimal process conditions that would yield the highest degradation efficiency for varying ATZ concentrations. Prediction of the optimal process conditions for practical applications supports adaptation of the Fe^{2+}-AP process to different ATZ concentrations encountered in the environment, thereby increasing the potential for maximum degradation. The results of this study may serve as a reference for the field application of the Fe^{2+}-AP process for remediation of ATZ contamination.

Acknowledgements

This study was funded by the Ministry of Science and Technology of Taiwan under Project No. 106-2221-E-005-009 -MY3. The authors acknowledge John F. Miano, Chief, Site Management Section, Bureau of Waste Site Clean-up, Department of Environmental Protection, Massachusetts, USA for valuable discussion and proofread of this manuscript.

Conflict-of-Interest Statement

The authors declare that they have no conflict of interest.

Author Contributions

X.T.H.L. (Ph.D. student) performed the data curation, formal analysis, investigation, methodology, software, validation, visualization, and wrote the original draft. C.L. (Professor) performed the conceptualization, formal analysis, methodology, supervision, project administration, wrote the original draft, reviewed and edited the manuscript.

References

1. Konstantinou IK, Hela DG, Albanis TA. The status of pesticide pollution in surface waters (rivers and lakes) of Greece. Part I. Review on occurrence and levels. *Environ. Pollut.* 2006;141: 555-570.
2. Huang J, Zhang H. Mn-based catalysts for sulfate radical-based advanced oxidation processes: A review. *Environ. Int.* 2019; 133:105141. https://doi.org/10.1016/j.envint.2019.105141
3. Wu S, Shen L, Lin Y, Yin K, Yang C. Sulfite-based advanced oxidation and reduction processes for water treatment. *Chem. Eng. J.* 2021;414:128872. https://doi.org/10.1016/j.cej.2021.128872
4. Yang J, Li J, Dong W, Ma J, Li T, Yang Y, Li J, Gu J. Deethylatrazine as a more appropriate hydroxyl radical probe compound during ozonation: Comparison with the widely used p-chlorobenzoic acid. *Chem. Eng. J.* 2016;295:443-450. https://doi.org/10.1016/j.cej.2016.03.014
5. Knusli E. History of the development of triazine herbicides. In: Gunther F.A., Gunther J.D. (Eds), Single Pesticide Volume: The Triazine Herbicides in Springer; 1970; New York. p. 1-9.
6. Solomon KR, Baker DB, Richards RP, Dixon KR, Klaine SJ, La Point TW, Kendall RJ, Weisskopf CP, Giddings JM, Giesy JP. Ecological risk assessment of atrazine in North American surface waters. *Environ. Toxicol. Chem.* 1996;15:31-76. https://doi.org/10.1002/etc.5620150105
7. USEPA. Decision Documents for Atrazine. Office of Prevention, Pesticide and Toxic Substances, Washington D.C., USA. United States Environmental Protection Agency (USEPA); 2006. https://ntrl.ntis.gov/NTRL/dashboard/searchResults/titleDetail/PB2006114876.xhtml
8. Hayes TB, Khoury V, Narayan A, Nazir M, Park A, Brown T, Adame L, Chan E, Buchholz D, Stueve T. Atrazine induces complete feminization and chemical castration in male African clawed frogs (Xenopus laevis). *Proc. Natl. Acad. Sci.* 2010; 107:4612-4617. https://doi.org/10.1073/pnas.0909519107
9. Ackerman F. The Economics of Atrazine. *Int. J. Occup. Environ. Health* 2007;13:437-445. https://doi.org/10.1179/oeh.2007.13.4.437
10. Thurman EM, Goolsby D, Meyer M, Kolpin DW. Herbicides in surface waters of the midwestern United States: The effect of spring flush. *Environ. Sci. Technol.* 1991;25:1794-1796. https://doi.org/10.1021/es00022a018
11. Bethsass J, Colangelo A. European Union bans atrazine, while the United States negotiates continued use. *Int. J. Occup. Environ. Health* 2006;12:260-267. https://doi.org/10.1179/oeh.2006.12.3.260
12. Gilliom RJ, Barbash JE, Crawford CG, Hamilton PA, Martin JD, Nakagaki N, Nowell LH, Scott JC, Stackelberg PE, Thelin GP. Pesticides in the Nation's Streams and Ground Water, 1992–2001. United State Geological Survey, Series Number 1291, Reston, Virginia, USA; 2006.
13. Le TP, Tran AT. Highly Hazardous Pesticides in Vietnam: A Situational Analysis. International Pollutant Elimination Network, Ho Chi Minh, Vietnam; 2020 [cited 10 March 2023]. Available from: https://ipen.org/documents/highly-hazardous-pesticides-vietnam-situational-analysis
14. Kolpin DW, Kalkhoff SJ, Goolsby DA, Sneck-Fahrer DA, Thurman EM. Occurrence of selected herbicides and herbicide degradation products in Iowa's ground water, 1995. *Ground Water* 1997;35:679-688. https://doi.org/10.1111/j.1745-6584.1997.tb00134.x
15. Kolpin D, Squillace P, Barbash J, Zogorski J. Pesticides and Volatile Organic Compounds in Shallow Urban Groundwater. Netherlands. A. A. Balkema Publishers; 1997. p. 469-474.
16. Gerecke AC, Schärer M, Singer HP, Müller SR, Schwarzenbach RP, Sägesser M, Ochsenbein U, Popow G. Sources of pesticides in surface waters in Switzerland: pesticide load through waste water treatment plants—current situation and reduction potential. *Chemosphere* 2002;48:307-315. https://doi.org/10.1016/S0045-6535(02)00080-2

17. Benotti MJ, Trenholm RA, Vanderford BJ, Holady JC, Stanford BD, Snyder SA. Pharmaceuticals and endocrine disrupting compounds in US drinking water. *Environ. Sci. Technol.* 2009;43:597-603. https://doi.org/10.1021/es801845a
18. Adams CD, Thurman E. Formation and transport of deethylatrazine in the soil and vadose zone. *J. Environ. Qual*. 1991;20: 540-547. https://doi.org/10.2134/jeq1991.00472425002000030007x
19. Kruger EL, Coats JR, Zhu BE. Relative mobilities of atrazine, five atrazine degradates, metolachlor, and simazine in soils of Iowa. *Environ. Toxicol. Chem.* 1996;15:691-695. https://doi.org/10.1002/etc.5620150512
20. Ribaudo M, Bouzaher A. Atrazine: Environmental Characteristics and Economics of Management. United States Department of Agriculture, Agricultural Economics Report No. 669, USA; 1994.
21. Readman J, Albanis T, Barcelo D, Galassi S, Tronczynski J, Gabrielides. Herbicide contamination of Mediterranean estuarine waters: results from a MED POL pilot survey. *Mar. Pollut. Bull.* 1993;26:613-619. https://doi.org/10.1016/0025-326X(93)90500-J
22. Chapman R, Stranger JW. Horticultural Pesticide Residues in Water: A Review of the Potential for Water Contamination by Pesticides Used in the Vegetable Industry in Victoria, Victoria. East Melbourne: Department of Food and Agriculture; 1992. p. 1-40.
23. Graymore M, Stagnitti F, Allinson G. Impacts of atrazine in aquatic ecosystems. *Environ. Int.* 2001;26:483-495. https://doi.org/10.1016/S0160-4120(01)00031-9
24. Ji Y, Dong C, Kong D, Lu J. New insights into atrazine degradation by cobalt catalyzed peroxymonosulfate oxidation: kinetics, reaction products and transformation mechanisms. *J. Hazard. Mater.* 2015;285:491-500. https://doi.org/10.1016/j.jhazmat.2014.12.026
25. Zheng W, Guo M, Chow T, Bennett DN, Rajagopalan N. Sorption properties of greenwaste biochar for two triazine pesticides. *J. Hazard. Mater.* 2010;181:121-126. https://doi.org/10.1016/j.jhazmat.2010.04.103
26. Shao S, Feng Y, Yu H, Li J, Li G, Liang H. Presence of an adsorbent cake layer improves the performance of gravity-driven membrane (GDM) filtration system. *Water Res.* 2017;108: 240-249. https://doi.org/10.1016/j.watres.2016.10.081
27. Sánchez V, López-Bellido FJ, Cañizares P, Rodríguez L. Assessing the phytoremediation potential of crop and grass plants for atrazine-spiked soils. *Chemosphere* 2017;185: 119-126. https://doi.org/10.1016/j.chemosphere.2017.07.013
28. Fan X, Song F. Bioremediation of atrazine: recent advances and promises. *J. Soils Sediments.* 2014;14:1727-1737. https://doi.org/10.1007/s11368-014-0921-5
29. Wols BA, Hofman-Caris CHM. Review of photochemical reaction constants of organic micropollutants required for UV advanced oxidation processes in water. *Water Res.* 2012;46: 2815-2827. https://doi.org/10.1016/j.watres.2012.03.036
30. Boczkaj G, Fernandes A. Wastewater treatment by means of advanced oxidation processes at basic pH conditions: A review. *Chem. Eng. J.* 2017;320:608-633. https://doi.org/10.1016/j.cej.2017.03.084
31. Miklos DB, Remy C, Jekel M, Linden KG, Drewes JE, Hübner U. Evaluation of advanced oxidation processes for water and wastewater treatment – A critical review. *Water Res.* 2018;139: 118-131. https://doi.org/10.1016/j.watres.2018.03.042
32. Kurian M. Advanced oxidation processes and nanomaterials-A review. *Cleaner Eng. Technol*. 2021;2:100090. https://doi.org/10.1016/j.clet.2021.100090
33. Liang C, Bruell CJ. Thermally activated persulfate oxidation of trichloroethylene: experimental investigation of reaction orders. *Ind. Eng. Chem. Res.* 2008;47:2912-2918. https://doi.org/10.1021/ie070820l
34. Zhang Y, Zhang Q, Dong Z, Hong J. Degradation of acetaminophen with ferrous/copperoxide activate persulfate: Synergism of iron and copper. *Water Res.* 2018;146:232-243. https://doi.org/10.1016/j.watres.2018.09.028
35. Kang Y-G, Hong S, Yoon H, Song I-G, Cho K, Chang Y-S. Mechanically combined persulfate on zerovalent iron: Mechanistic insights into reduction and oxidation processes. *Chem. Eng. J.* 2021;414:128772. https://doi.org/10.1016/j.cej.2021.128772
36. Fordham J, Williams HL. The persulfate-iron (II) initiator system for free radical polymerizations1. *J. Am. Chem. Soc*. 1951;73:4855-4859. https://doi.org/10.1021/ja01154a114
37. Kolthoff I, Miller I. The chemistry of persulfate. I. The kinetics and mechanism of the decomposition of the persulfate ion in aqueous medium1. *J. Am. Chem. Soc*. 1951;73:3055-3059. https://doi.org/10.1021/ja01151a024
38. Samy M, Alalm MG, Khalil MN, Ezeldean E, El-Dissouky A, Nasr M, Tawfik A. Treatment of hazardous landfill leachate containing 1, 4 dioxane by biochar-based photocatalysts in a solar photo-oxidation reactor. *J. Environ. Manage.* 2023;332: 117402. https://doi.org/10.1016/j.jenvman.2023.117402
39. Samy M, Kumi AG, Salama E, ElKady M, Mensah K, Shokry H. Heterogeneous activation of persulfate by a novel nano-magnetite/ZnO/activated carbon nanohybrid for carbofuran degradation: Toxicity assessment, water matrices, degradation mechanism and radical and non-radical pathways. *Process Saf. Environ. Prot.* 2023;169:337-351. https://doi.org/10.1016/j.psep.2022.11.038
40. Samy M, Mensah K, El-Fakharany EM, Elkady M, Shokry H. Green valorization of end-of-life toner powder to iron oxide-nanographene nanohybrid as a recyclable persulfate activator for degrading emerging micropollutants. *Environ. Res.* 2023;223:115460. https://doi.org/10.1016/j.envres.2023.115460
41. Mensah K, Samy M, Ezz H, Elkady M, Shokry H. Utilization of iron waste from steel industries in persulfate activation for effective degradation of dye solutions. *J. Environ. Manage.* 2022;314:115108. https://doi.org/10.1016/j.jenvman.2022.115108
42. Aman A, Bhardwaj R, Gahlot P, Phanden RK. Selection of cutting tool for desired surface finish in milling Machine using Taguchi optimization methodology. *Mater. Today: Proc.* 2023;78:444-448. https://doi.org/10.1016/j.matpr.2022.10.253
43. Bakhbergen U, Shon C-S, Zhang D, Kim JR, Liu J. Optimization of mixture parameter for physical and mechanical properties of reactive powder concrete under external sulfate attack using Taguchi method. *Constr. Build. Mater.* 2022;352:129023. https://doi.org/10.1016/j.conbuildmat.2022.129023
44. Geerts GA, Overturf J-H, Oberholzer TG. The effect of different reinforcements on the fracture toughness of materials for inter-

im restorations. *J. Prosthet. Dent.* 2008;99:461-467. https://doi.org/10.1016/S0022-3913(08)60108-0
45. Arunkumar S, Prabha C, Saminathan R, Khamaj JA, Viswanath M, Ivan CKP, Subbiah R, Kumar PM. Taguchi optimization of metal inert gas (MIG) welding parameters to withstand high impact load for dissimilar weld joints. *Mater. Today: Proc.* 2022; 56:1411-1417. https://doi.org/10.1016/j.matpr.2021.11.619
46. Zeng M, Tang L, Lin M, Wang Q. Optimization of heat exchangers with vortex-generator fin by Taguchi method. *Appl. Therm. Eng.* 2010;30:1775-1783. https://doi.org/10.1016/j.applthermaleng.2010.04.009
47. Wang X, Wang Y, Chen N, Shi Y, Zhang L. Pyrite enables persulfate activation for efficient atrazine degradation. *Chemosphere* 2020;244:125568. https://doi.org/10.1016/j.chemosphere.2019.125568
48. Rao Y, Qu L, Yang H, Chu W. Degradation of carbamazepine by Fe (II)-activated persulfate process. *J. Hazard. Mater.* 2014;268:23-32. https://doi.org/10.1016/j.jhazmat.2014.01.010
49. Criquet J, Leitner NKV. Degradation of acetic acid with sulfate radical generated by persulfate ions photolysis. *Chemosphere* 2009;77:194-200. https://doi.org/10.1016/j.chemosphere.2009.07.040
50. Liang C, Lee IL. In situ iron activated persulfate oxidative fluid sparging treatment of TCE contamination — A proof of concept study. *J. Contam. Hydrol.* 2008;100:91-100. https://doi.org/10.1016/j.jconhyd.2008.05.012
51. Chawla OP, Fessenden RW. Electron spin resonance and pulse radiolysis studies of some reactions of peroxysulfate ($SO_4^{\cdot -1,\ 2}$). *Phys. Chem.* 1975;79:2693-2700. https://doi.org/10.1021/j100591a020
52. Liang C, Bruell CJ, Marley MC, Sperry KL. Persulfate oxidation for in situ remediation of TCE. I. Activated by ferrous ion with and without a persulfate–thiosulfate redox couple. *Chemosphere* 2004;55:1213-1223. https://doi.org/10.1016/j.chemosphere.2004.01.029
53. Miller CJ, Rose AL, Waite TD. Importance of iron complexation for Fenton-mediated hydroxyl radical production at circumneutral pH. *Front. Mar. Sci.* 2016;3:134. https://doi.org/10.3389/fmars.2016.00134
54. Neta P, Huie RE, Ross AB. Rate constants for reactions of inorganic radicals in aqueous solution. *J. Phys. Chem. Ref. Data* 1988;17:1027-1284. https://doi.org/10.1063/1.555808
55. Pignatello JJ, Oliveros E, MacKay A. Advanced oxidation processes for organic contaminant destruction based on the Fenton reaction and related chemistry. *Crit. Rev. Environ. Sci. Technol.* 2006;36:1-84. https://doi.org/10.1080/10643380500326564
56. Jiang Z, Zhang X, Wang Z, Cao B, Deng S, Bi M, Zhang Y. Enhanced biodegradation of atrazine by Arthrobacter sp. DNS10 during co-culture with a phosphorus solubilizing bacteria: Enterobacter sp. P1. *Ecotoxicol. Environ. Saf.* 2019;172: 159-166. https://doi.org/10.1016/j.ecoenv.2019.01.070
57. House DA. Kinetics and mechanism of oxidations by peroxydisulfate. *Chem. Rev.* 1962;62:185-203. https://doi.org/10.1021/cr60217a001